MODELING THE STABLE ATMOSPHERIC BOUNDARY LAYER WITH A THIRD-ORDER CLOSURE MODEL

Anning Cheng*[1,2], and Kuan-Man Xu[1]
[1]NASA Langley Research Center, [2]Hampton University

1. Introduction

The stable atmospheric boundary layer (ABL) plays an important role in the transfers of momentum, heat and mass between the Earth's surface and the atmosphere. The ABL is usually stable between sunset and sunrise. The stable ABL is shear-driven and has different properties than the convective ABL. It is difficult for global models to simulate the stable ABL over lands. Mean surface air temperature can differ by more than 10 K by slightly changing the mixing scheme. The GEWEX (Global Energy and Water Cycle Experiment) Atmospheric Boundary Layer Study (GABLS) initiative is designed to improve the prediction of stable ABLs in atmospheric models (Holtslag 2003).

Although third-order turbulence closure models have successfully simulated the convective ABLs (e.g. Bougeault 1981; Krueger 1988; Lappen and Randall 2001; Golaz et al. 2002; Cheng and Xu 2004), the stable ABLs have rarely been studied with a third-order closure model. On the other hand, Weng and Taylor (2003) showed that 1.5-order closure models and 2nd-order closure models have similar behavior for most stable ABL cases although fully 2nd-order closure models have significant advantages for some situations such as flow over hills. They also found that the specification of turbulence length scale can significantly impact the simulated results in all turbulence closure models. Cuxart et al. (2004) found that 1.5-order closure models produce less mixing than the first-order closure models.

This study presents some preliminary results from a third-order closure model to simulate a stable ABL case. Both advantages and disadvantages of the third-order closure model are discussed in this study by compared it with a 1.5-order closure model.

2. Case description and model configuration

This case is based upon the simulations presented by Kosovic and Curry (2000) for the stable Arctic ABL. The ABL is driven by an imposed geostrophic wind and a specific surface cooling. The shear production of the turbulent kinetic energy (TKE) is positive, while the buoyancy production is negative. It is a typical stable ABL case. The boundary-layer height is between 150 m and 250 m when the ABL reaches a quasi-steady state at 9 h. This case has been used for a Large-Eddy Simulation (LES) intercomparison (Beare et al, 2004) and single column model (SCM) intercomparison (Cuxart et al. 2004) with the aim to test the ability of LESs and SCMs to simulate the stable ABL.

The partially prognostic third-order closure model by Cheng and Xu (2004) is used in this study. The model assumes joint double Gaussian distributions of vertical velocity, temperature and moisture. The first and second moments of all variables as well as the third moments of vertical velocity, liquid-water potential temperature and total water mixing ratio are predicted to determine a proper probability density function (PDF). Once the PDF is known, the rest of the third moments and all fourth moments are diagnosed.

The momentum turbulent flux is calculated by the K-theory

$$\overline{u'w'} = -K_m \frac{\partial U}{\partial z}, \text{ and} \tag{1}$$

$$\overline{v'w'} = -K_m \frac{\partial V}{\partial z}, \tag{2}$$

where $K_m = \alpha l e^{0.5}$ is the eddy viscosity or turbulence diffusion coefficient, $\alpha = 0.15$ is a constant, l is the dissipation length scale, and $e = \frac{1}{2}(\overline{u'^2} + \overline{v'^2} + \overline{w'^2})$ is the TKE. The three components ($\overline{u'^2}$, $\overline{v'^2}$ and $\overline{w'^2}$) of the TKE are predicted by

$$\frac{\partial \overline{u'_i u'_i}}{\partial t} = P_t + P_{df} + P_s + P_b + P_r + P_{ds}, \tag{3}$$

where P_t P_{df}, P_s, P_b, P_r and P_{ds} are the terms that represent transportation, diffusion, shear production, buoyancy production, pressure redistribution and dissipation of $\overline{u'_i u'_i}$, respectively. The potential temperature flux is predicted by

$$\frac{\partial \overline{w'\theta'}}{\partial t} = p_t + p_{df} + p_s + p_b + p_{ds}, \tag{4}$$

where p_t p_{df}, p_s, p_b, and p_{ds} are the terms that represent transportation, diffusion, shear production, buoyancy production, and dissipation of $\overline{w'\theta'}$, respectively. Weng and Taylor (2003) did not predict the potential temperature flux, but diagnosed it from the K-theory when the 2nd-order closure was used. This is one of the differ-

* Corresponding author address: Dr. Anning Cheng, NASA Langley Research Center, Mail Stop 420, Hampton, VA 23681.

ences between this study and theirs. The third moment terms are very small and can be neglected for this case. Thus, the equations are not discussed here.

The 1.5-order closure model used in this study only predicts the TKE and does not distinguish among its three components. All the fluxes are diagnosed using the K-theory. Further details of the model can be found in Xue et al. (2000).

Both the 1.5-order and third-order models are run in 1-D. A vertical domain of 400 m with uniform grid size of 6.25 m is used. The time step for the 1.5-order closure is 10 s, while that for the third-order closure is 0.2 s. This is a huge disadvantage of the third-order closure model. The higher-moment equations can become unstable using large time steps. The latitude is 73° N and a constant geostrophic wind of 8 m s^{-1} is prescribed. For the lowest 100 m, θ =265 K and then it increases at 0.01 K m^{-1} to the domain top. The surface temperature is 265 K initially and decreases at a rate of 0.25 K h^{-1} throughout the integration. For further details of the model configuration, please see Cuxart et al. (2004).

3. Results

The time evolutions of the friction velocity (a), Obukhov Length (b) and boundary layer height (c) are shown in Fig. 1. Note that the solid line is for the third-order model and the dotted line is for the 1.5-order model in all the figures except Figs. 4a and 5. The third-order closure model predicts a larger friction velocity and a higher PBL top, but a smaller Obukhov length than the 1.5-order model.

The maximum mean u (Fig. 2a) and v (Fig. 2b) wind components at 9 h for the third-order closure model are located at higher levels than the 1.5-order closure model. The potential temperature increases more rapidly from the surface to near 200 m (Fig. 2c) and is mixed more efficiently in the boundary layer for the 1.5-order closure model. This is because the dissipation length

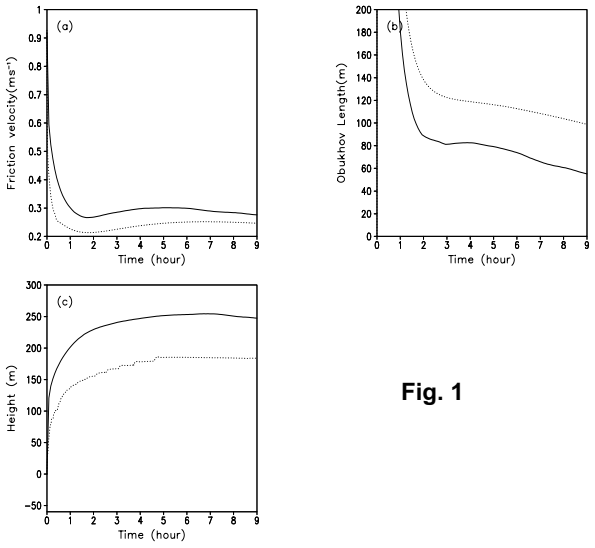

Fig. 1

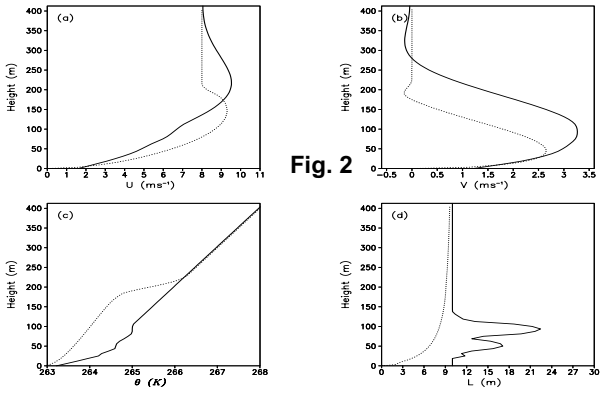

Fig. 2

scale or the mixing length scale for the 1.5-order closure model (Fig. 2d) is much smaller than the third-order closure model.

The vertical behavior of the mean wind components can be explained by the turbulent momentum fluxes at their respective directions (Figs. 3a, and b). The third-order closure model predicts larger turbulent momentum fluxes and the maximum fluxes appear at higher levels. The turbulent momentum fluxes are calculated by the K-theory, Eqs. (1) and (2), as in the 1.5-order closure model. Why are the momentum fluxes from the third-order closure model larger than those from the 1.5-order closure model? This is because the mixing length from the third-order closure model is much larger than that from the 1.5-order closure model (Fig. 2d) although the TKE also impacts the momentum fluxes. The potential temperature flux from the third-order closure model varies rapidly with height below 75 m but slowly above 75 m, compared with a nearly constant variation with height in the 1.5-order closure model (Fig. 3c). The maximum TKE from the third-order closure model that occurs near the surface is smaller than that from the 1.5-order closure model (Fig. 3d) although the friction velocity of the third-order closure model is larger (Fig. 1a)

The TKE components from the third-order model are shown in Fig. 4a. $\overline{u'^2}$ (solid) has the highest values,

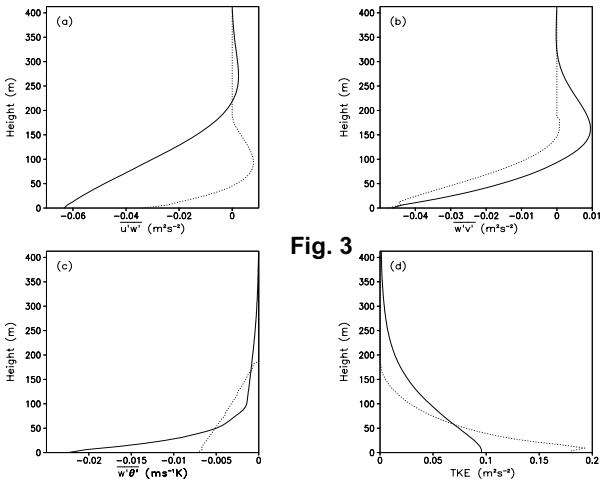

Fig. 3

while $\overline{w'^2}$ (long dashed) has the smallest values. The third-order closure model can capture such anisotropy well. Shear production of the TKE budget is positive (Fig. 4b), but buoyancy production is negative (Fig. 4c). Note that for the $\overline{w'^2}$ equation, shear production ($-2\overline{w'w'}\frac{\partial \bar{w}}{\partial z}$) is almost zero while buoyancy production is negative. Shear production ($-\overline{u'w'}\frac{\partial \bar{v}}{\partial z}-\overline{v'w'}\frac{\partial \bar{u}}{\partial z}$) is positive but buoyancy production is zero in the $\overline{u'^2}$ and $\overline{v'^2}$ equations. So $\overline{w'^2}$ is mainly produced by the pressure redistribution, that is, the $\overline{w'^2}$ is mainly converted from $\overline{u'^2}$ and $\overline{v'^2}$. The third-order closure models developed by Lappen and Randall (2001) and Golaz et al. (2002) for convective ABL only predict $\overline{w'^2}$. These model will not produce reasonable TKE for the stable ABL unless the equations of $\overline{u'^2}$ and $\overline{v'^2}$ are added.

As mentioned earlier, the third-order closure model produces less mixing of potential temperature than the 1.5-order closure model does although its potential temperature flux near the surface is larger. The reason is that the buoyancy production of potential temperature flux is positive and dominates the other terms in Eq. (4). The buoyancy term ($p_b = \beta\overline{\theta'\theta'}_v \approx \beta\overline{\theta'\theta'}$) is shown by the dotted line in Fig. 5 while the solid line represents the sum of all the other terms for the $\overline{w'\theta'}$ equation. The effects of moisture are very small, so the buoyancy production of $\overline{w'\theta'}$ is always positive, which inhibits the mixing. When the 1.5-order closure model calculates $\overline{w'\theta'}$ from the K-theory, the buoyancy effects are totally neglected, which result in larger transport of potential temperature and larger mixing of potential temperature.

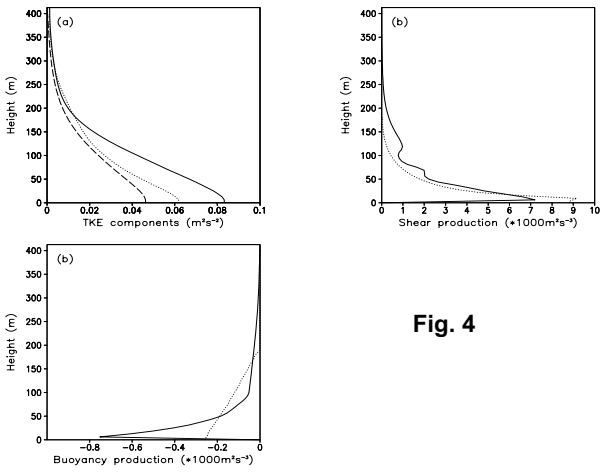

Fig. 4

Fig. 5

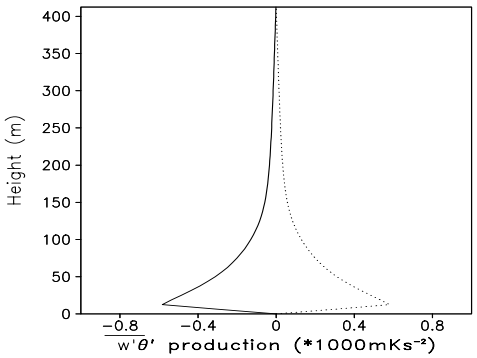

4. Discussion and conclusions

A third-order closure model has been used to simulate the GABLS case in this study. The vertical profiles of the TKE, TKE components, fluxes and the mean temperature and wind components have been compared with those produced by a 1.5-order closure model. There are significant differences in these profiles between the two models. The smaller mixing of potential temperature of the third-order closure model is due to the positive buoyancy in the $\overline{w'\theta'}$ equation. The difference from the 1.5-order model is related to the difference in the dissipation length scales. In addition, the horizontal TKE components ($\overline{u'u'}$ and $\overline{v'v'}$) from the third-order closure model are larger than the vertical component ($\overline{w'w'}$), which is consistent with results from LESs. However, the 1.5-order closure model cannot predict this anisotropy in TKE. Despite of the significant improvement in the results, the computational cost of the third-order closure model is much higher than the 1.5-order closure model.

Acknowledgments: This research was partially supported by the Environmental Sciences Division of the U.S. Department of Energy as part of the Atmospheric Radiation Measurement Program, under interagency agreement DE-AI02-02ER63318 to NASA Langley Research Center.

References

Bougeault, P., 1981: *J. Atmos. Sci.,* **38,** 2429-2439.

Beare, R. J. and coauthors, 2004: submitted to *Boundary-layer Meteorol*.

Cheng, A. and K.-M. Xu, 2004: in preparation for *J. Atmos. Sci.*

Cuxart, J. and coauthors, 2004: in preparation for *Boundary-layer Meteorol*.

Golaz, J.-C., V. E. Larson, and W. R. Cotton, 2002: *J. Atmos. Sci.,* **59,** 3540-3551.

Holtslag, A. M., 2003: *GEWEX WCRP News*, **13**, 7-8.

Kosovic, B. and J. A. Curry, 2000: *J. Atmos. Sci.,* **57,** 1052-1068.

Krueger, S. K., 1988: *J. Atmos. Sci.,* **45,** 2221-2250.

Lappen, C.-L., and D. A. Randall,2001: *J. Atmos. Sci.,* **58,** 2021-2036.

Weng, W. and P. A. Taylor, 2003: *Boundary-layer Meteorol*, **107**, 371-400.

Xue, M., K. K. Drogemeiri, and V. Wong, 2000: *Meteor. Atmos. Phys.,* **75**, 161-193.